Zoomorphology (1984) 104:204–215

Zoomorphology

Model studies on the mechanical significance of grouping in compound spider slit sensilla (Chelicerata, Araneida)

Friedrich G. Barth[1], **Elmar Ficker**[2] **and Hans-Ulrich Federle**[2]

[1] Gruppe Sinnesphysiologie, Zoologisches Institut der Universität, Siesmayerstr. 70, D-6000 Frankfurt a.M., Federal Republic of Germany

[2] Lehrstuhl C für Mechanik und Spannungsoptik, Technische Universität München, Arcisstr. 21, D-8000 München, Federal Republic of Germany

Summary. The mechanical implications of various types of slit arrangements found among the strain-sensitive slit sensilla in the arachnid exoskeleton (Fig. 3) were studied by measuring the deformation of model slits, cut into plastic discs, under static load applied in the plane of the disc and from varying directions (Figs. 1, 2).

1. Close parallel, *lyriform arrangements*. Compression of slits (adequate stimulus) reaches much higher values than dilatation. It is highest with the load direction at right angle to the slit axes. Also, in the majority of slits the range of load angles resulting in compression is considerably larger than that leading to dilatation. Length distribution and lateral shift of slits in the models have a pronounced effect on slit deformability (Figs. 4–5): (a) In the "oblique bar" arrangement with slits of equal length and regular lateral shift (Fig. 4A) deformation of all slits is very similar at all load directions. In all slits compression results from a range of load angles larger than 120°. (b) In arrangements with a regular increase in slit length and a triangular outline shape deformability differs greatly among the slits at all load angles (Fig. 4B). (c) The slit configuration with a heartshaped outline (Fig. 4C) is peculiar for the large spread of load angles at which the compression of the different slits is highest. – These properties recommend different arrangements for the solution of different strain measuring problems, with for instance, the particular need of a wide *angular working range* (arrangement *a*), of a large *spectrum of absolute sensitivities* (*b*), or of the *analysis of load direction* (*c*).

2. *Angle* and *distance* between slits. Due to the mechanical directionality inherent in an elongated slit the divergence of slit axes within a group of slits is likely to indicate the importance of the analysis of strain direction (Fig. 6). The mechanical interaction between closely neighbouring slits decreases with their distance from each other. In a parallel arrangement of equally long slits it disappears if the distance is about 1.5 times the slit length (Fig. 7).

3. Aiming towards a *mechanical model* which would explain the complex deformation found in a lyriform organ, we consider the outline of the organ as a hole traversed by beams of material. Slit deformation can be calculated from the elastic lines of the beams which separate the slits and information drawn from photoelastic experiments (Figs. 8–11).

Correspondence and offprint requests to: F.G. Barth

A. Introduction

Much has been learned in recent years about the principles underlying the sensory measurement of strains in the arthropod exoskeleton and its biological significance. (Barth 1976, 1981; Barth and Blickhan 1984). One of the gaps in our knowledge concerns the functional relevance of the striking richness of patterns of arrangement. In particular this applies to the "lyriform" arrangements, with several slit sensilla lying closely side by side, typical of the araneids (Barth and Libera 1970; Barth and Wadepuhl 1975; Barth and Stagl 1976).

So far details of both the mechanical *and* physiological implications of its slit arrangement have been studied in only one example of such a compound organ, i.e. lyriform organ HS8 on the posterior aspect of the spider leg tibia (Barth and Pickelmann 1975; Barth and Bohnenberger 1978; Bohnenberger 1981). Among the most important findings was a pronounced difference in absolute sensitivity among its slits and a considerable increase of the linear working range of the compound arrangement as compared to a single slit.

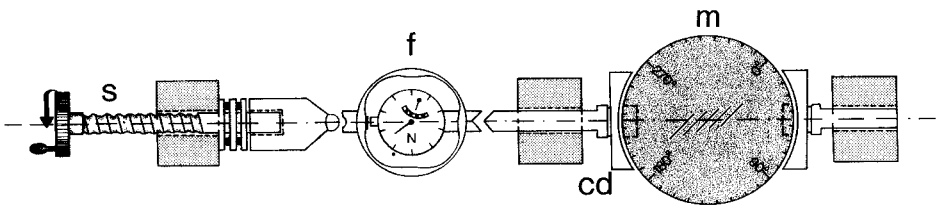

Fig. 1. Apparatus used to load the models. Both model *m* and force gauge *f* were held by clamping device *cd* mounted on a V-way. Force was applied by turning the screw *s*. Markings on the model allowed precise adjustment of load angle α by rotating the model disk into its desired position before loading it

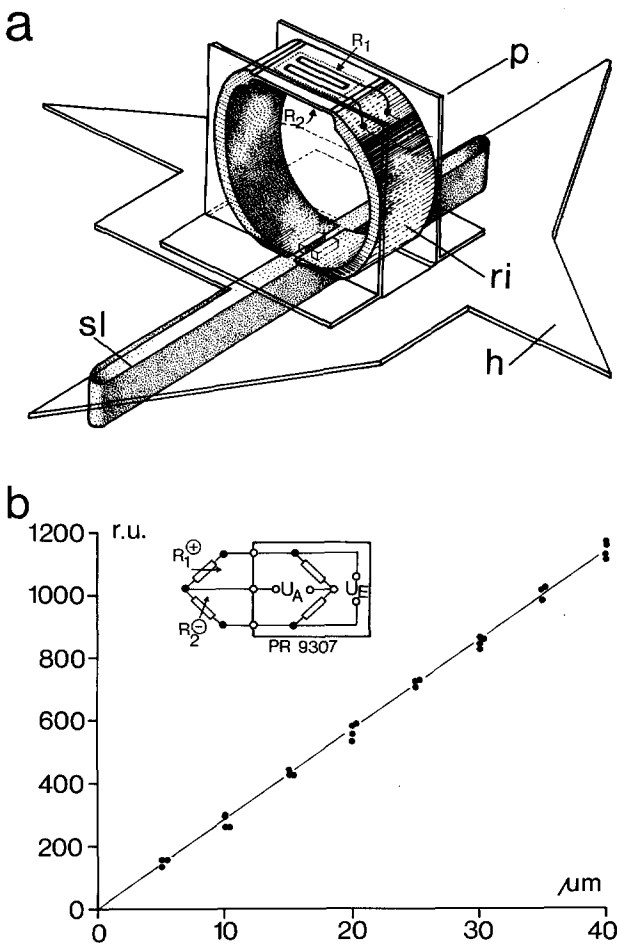

Fig. 2. a. Device to measure slit deformation. The metal torus *ri*, with strain gauges R_1 and R_2 attached to both surfaces of its thin and flat upper part, is inserted into the model slit *sl* with the small ridges bordering the cut at its lower part. Deformation of the slit changes the width of the cut in the torus and as a consequence the resistance of the strain gauges. Transparent devices perpendicular (*p*) and horizontal (*h*) to the model disk serve to align the torus precisely with respect to the slit axis and the point along its length to be measured. **b** Calibration of the torus shown in a. Inset: position of strain gauges R_1 and R_2 in the Wheatstone bridge circuit. U_A, output voltage plotted as relative units *r.u.* as a function of the change in the width (µm) of the cut in the torus

The multitude of arrangements generally found among the slit sensilla of arachnids can be reduced to a small number of basic configurations. The purpose of the present paper is to investigate the main mechanical implications of these configurations under static load, using plastic models. We first describe how slit arrangement and load angle affect the deformation of the model slits and then explain our results using beam theory and information gained from photoelastic experiments.

B. Material and methods

Models made from carefully annealed Araldite B or Plexiglass were used for deformation measurements and to determine the isochromatics and isoclinics in photoelastic experiments. They were disks 260 mm in diameter and 6 mm thick. When the slits were cut into them care was taken to avoid initial stresses persisting in the absence of external load. Slit lengths varied between 10 and 50 mm according to the type of lyriform organ modelled. Slit width was always 2 mm. The types of slit arrangements modelled were chosen to examine the mechanical relevance (i) of the main types of slit arrangements found among the lyriform slit sense organs (Figs. 3, 4), (ii) of the angle formed by neighbouring slits (Fig. 6), and (iii) of the distance between neighbouring slits (Fig. 7).

Static load was applied to the carefully aligned disks in their plane with the apparatus shown in Fig. 1, which has been used before in a similar form (Barth 1972a). Precautions were taken (and their effects tested by means of photoelasticity) to provide for a homogeneous introduction of the load into the disk. The areas directly loaded (and facing each other) covered 942 mm^2 each, corresponding to an angle of 70°. The applied force was monitored with a force gauge (Tiedemann 1290) measuring the deformation of a metal torus. It measured 608 N, the resulting mean pressure being 0.64 N/mm^2. By using such relatively small forces bending of the disk was avoided, as can be seen from the isochromatic fringe pattern. Load direction was varied by rotating the disk in steps of 15° before loading it.

To measure both *slit compression* and *slit dilatation* a metal torus (similar to the one used by Barth and Pickelmann 1975), thin and flat at one side and cut open on the opposite side, was used (Fig. 2). When inserted into a model slit with the ridges along its cut, the changing slit width caused opening or closing of the torus. This was measured by a pair of strain gauges glued to either side of the flattened part of the torus. Thereby differential measurement increased the sensitivity of the device. The strain gauges were arranged to form parts of a Wheatstone bridge (Philips carrier frequency bridge PR 9307). A digital voltmeter monitored the signal from the bridge. Due to the great compliance of the ring mechanical interference with the slit was negligible. Both compression and dilatation of a model slit could be measured by inserting the torus in a slightly pre-compressed state. The whole system was calibrated and checked for linearity with the light microscope (Fig. 2).

All deformation values are expressed in relative units. They can be converted into µm by multiplication with $k = 3.5 \times 10^{-2}$. Measurements were well reproducible provided the measuring ring was carefully aligned parallel to the slit at the various measuring positions. A plastic device was used to orient the ring precisely along reference lines drawn onto the model (Fig. 2). Slit deformation was measured at four points (A to D) equidistant along the slit's length and at a point corresponding to the dendrite attachment site in the original slit membrane (Barth and Libera 1970; Barth and Stagl 1976).

Photoelastic techniques were conventional (Föppl and Mönch 1972). We used a reflexion polariscope (Tiedemann) to enhance the optical effect of the strains. Whereas Plexiglass models were mainly used for the deformation measurements, the isochromatics were determined in Araldite models. Also, the loads applied were higher in case of the Araldite models. The deformation of the Araldite models can easily be calculated from that of the Plexiglass models by introducing a factor which derives from the direct proportionality between deformation and load and inverse pro-

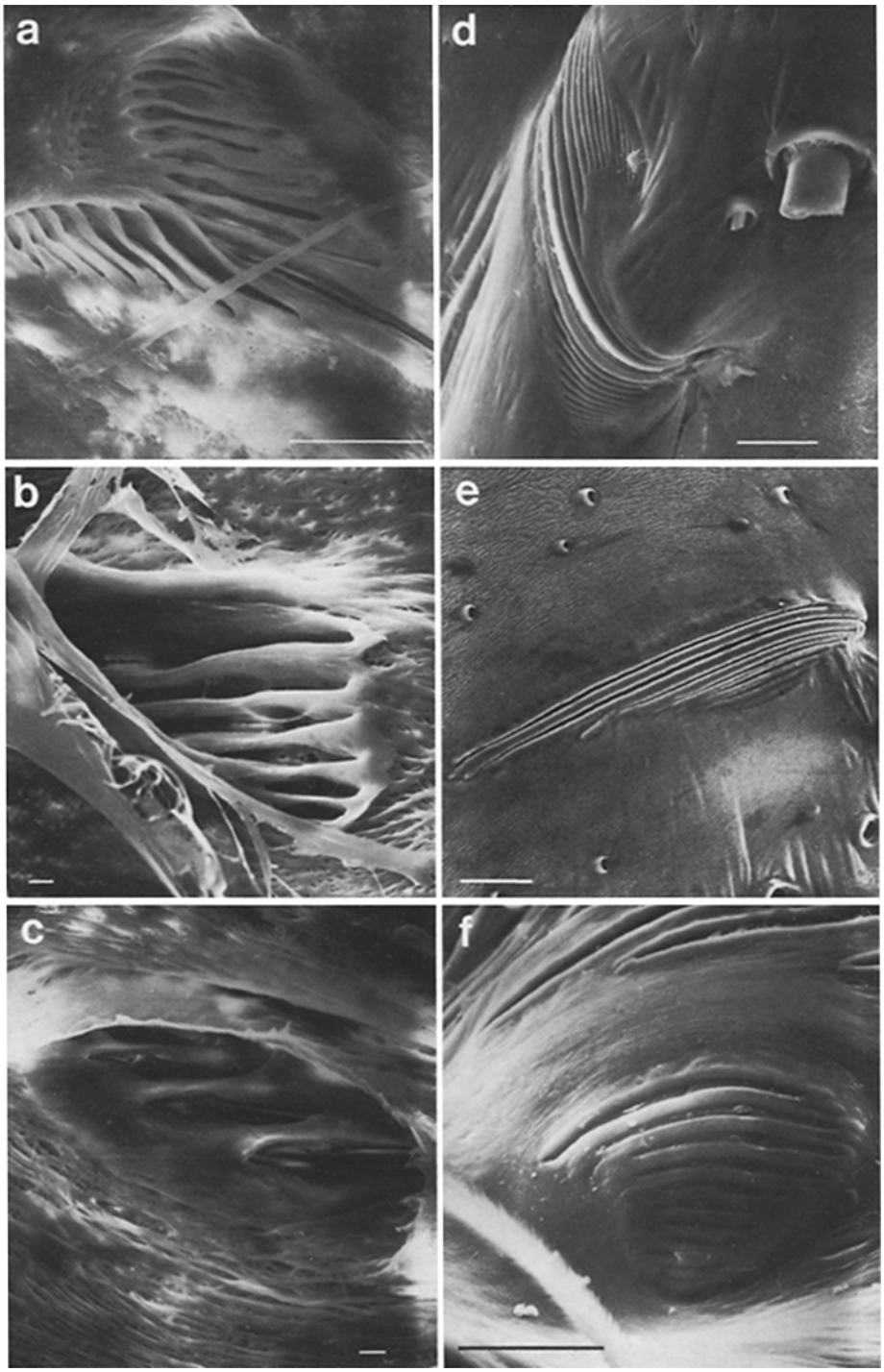

Fig. 3a–f. Examples of lyriform organs (compound slit sensilla) showing principal types of slit arrangement. In **a–c** exuviae were photographed from inside, whereas in **d–f** lyriform organs are shown as seen from the outside (legs of adult spiders, *Cupiennius salei*). **a** and **f** are found on the trochanter (compare models C and B1), **b** and **e** on the tibia (compare models B2 and B3), and **c** and **d** on the femur (compare models A and B3). Scale: 5 μm in b and c; 50 μm in a, d and f, and 40 μm in e

portionality between deformation and Young's modulus. For arguments concerning the material, shape and loading of the models see Barth (1972a).

C. Results

I. Compound "Lyriform" Arrangements

1. General

Although the shapes of arachnid lyriform organs vary in detail they can be classified into only a few characteristic arrangements of slits. These differ with respect to the degree of lateral shift between the neighbouring slits and to the distribution of slit lengths within the group (Fig. 3). While the number of slits in the original lyriform organs ranges from 2 to 29, five slits were chosen for all models in order not to obscure the effect of *arrangement* and *length distribution*. The five model arrangements chosen here are best described by their outline shape (Fig. 4, left column): *A "oblique bar"*, with all slits of equal length and constant lateral shift; *B* three *"triangular"* configurations, with the same graduated lengths of slits 1–5, but differences in lateral shift (*B1*, isosceles triangle with gradual change in slit

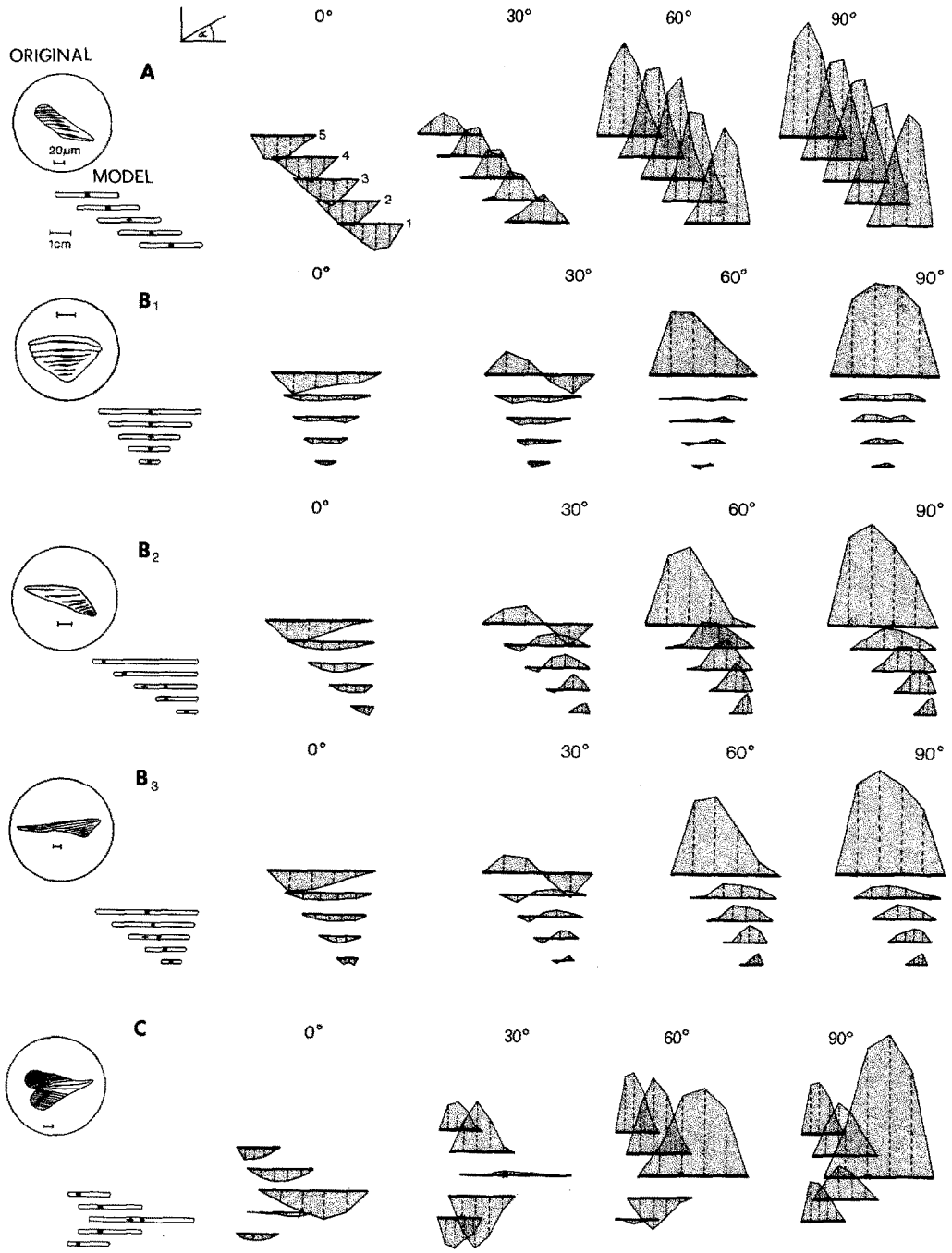

Fig. 4. Deformation of model slits arranged in groups of five according to the five principal original arrangements (A–C, left). Deformation of the slits is given for four points along their length and for four load angles α: 0° (parallel to slits), 30°, 60° and 90°. Compression values are plotted above the thick line symbolizing the slit, whereas slit dilatation points downward. For position of original lyriform organs shown as insets see Barth and Libera (1970)

length; *B2*, rectangular triangle; *B3*, scalene triangle); *C* *"heart"*, with the longest slit in the middle and shorter ones on both sides. Figure 3 shows typical examples of original compound organs; for more details see the literature (Barth and Libera 1970; Barth and Wadepuhl 1975; Barth and Stagl 1976).

2. Deformation of slits

Deformation along entire slit. The following conclusions can be drawn from Fig. 4 which gives the deformation values for four load angles (0°, which equals the orientation of slits, 30°, 60°, 90°)[1].

a) In all cases compression, which is the adequate stimulus in the original slit sensillum, reaches much higher absolute values than dilatation. Dilatation, even at its maximum,

[1] Load angle was changed in steps of 15°. In models *B2*, *B3* and *C* where the loading situation at α is different from that at $180°-\alpha$ (except at $\alpha=0°$), it covered the range from 0° to 165°. Only four values of α are given here because they suffice to show the essentials.

measures only between one-third and one-fifth of the largest values found for compression.

b) The angular ranges of load direction resulting in compression and dilatation, respectively, vary greatly among the five models. Whereas in model *A* simultaneous compression of all slits results from load directions varying at least between[2] 30° and 150°, the corresponding range is only from about 75° to 105° in models *B1* and *C*. Models *B2* and *B3* are in between.

c) The highest compression value found among the slits in each model results from a load direction of 90°. The angular range with high compression values, however, extends down to about 45° and up to about 150°, where compression values are still roughly twice as large as the maximum values found for any dilatation in the same model (in model *C* this range is slightly smaller).

d) Only in model *A* do the slits behave nearly uniformly at all load angles. They are all either dilated or compressed by nearly the same amount, the only difference being the site of maximum deformation. In all other model configurations the slits of a group do not behave alike: some are actually compressed while others are dilated at the same load angle. In the triangular configuration (*B1, B2, B3*) deformation of the longest peripheral slit always exceeds that of all the others.

Ratios of peak compression of this slit and the next in magnitude of deformation range, depending on load direction, are from 4 to 16 in model *B1*, from 1.5 to 10 in model *B2*, and from 3 to 11 in model *B3*. The corresponding values for dilatation are 1 to 3 (*B1*), 1.5 to 4 (*B2*), and 2 to 4 (*B3*). Model C is more complex in this respect: Again the longest slit, which has the center position in the group, is the one with greatest deformation; there are load directions, however, at which deformation of one or both of the slits next to it on the same side is larger (at 15°–45°, and 135°–165°).

e) Transition from dilatation to compression occurs at load angles from 15° to 30° ($180-\alpha$). Whereas in configuration *A* the sign of the deformation changes simultaneously in all slits, the process is more complex in configuration *C*. In this model the central slit is compressed (dilated) while two of its neighbours on the same side are dilated (compressed) at load angles between 15° and 60° (120°–165°, respectively). In addition, deformation of the two neighbouring slits "switches sides" at load angles between 15°–30°, and 150°–165°. The triangular configurations (*B*), on the other hand, are more complex with respect to the heterogeneity of the deformation of individual slits. In particular at load directions between 30°–45° and 135°–165° the slits are compressed towards one end and at the same time dilated towards the other.

f) The site of maximum deformation of a slit is by no means always in the middle as in the case of single, isolated slits (Barth and Pickelmann 1975). Its position varies with (i) the position of a particular slit in a specific group, (ii) the load direction, and (iii) the type of slit configuration. In general, change of load direction does not much alter the distribution of the sites of maximum compression if it is between 75° and 105°. At other angles, however, changes as small as 15° or less may result in considerable shifts.

Deformation at dendrite attachment site. Deformation at that point in the slit which corresponds to the dendrite attachment site in the original is of particular interest, since this is where slit compression triggers the nervous response. In all models examined here the dendrite area (location see Barth and Libera 1970, Barth and Stagl 1976) lies just in that region of the slit where the largest values of compression are found. Fig. 5a shows the deformation of this area only for all slits in models *A, B1*, and *C* as a function of load direction:

a) The "oblique bar" model (*A*) is outstanding for its homogeneity among the slits and the high values of compressional deformation in all of them at load angles around 90°. The main feature of the "triangular" arrangement (*B1*) is the great difference between the longest and all other slits. The "heart" configuration's (*C*) peculiarity is the large difference between the slits in the angular range of load giving the highest compression values.

b) The angular range of load directions resulting in compression is largest for configuration *A* (145°). The smallest ranges are found in slits of configuration *C* (105°). As a whole, however, arrangement *C* covers almost the full range of 180° with at least one slit being compressed at a particular load angle. In all other models this range is smaller.

c) A comparison among the three triangular arrangements (Figs. 5a, b; equal length of corresponding slits 1–5) shows that even small changes in slit position have a pronounced effect on the deformation pattern. Due to the shift of slits 1–4 towards one end of slit 5 the load angle ranges resulting in compression are larger in model *B3* than in model *B1*. The difference amounts to about 20° in the longest slit (5) and to about 35° in the shortest one (1). Also, the amount of compression is doubled to tripled in slits 1–4 and its maximum shifted from a load angle of 90° to one between 60° to 75°.

II. Variation of angle and distance between slits

1. Angle

General. Due to the elongated shape of slit sensilla their deformation and consequently their sensitivity is highly directional (Barth 1972a, b; 1981) with maximum deformation usually found at load directions between 75° and 105°. Using photoelastic techniques it was shown that lyriform organ HS8 on the tibia (an organ representative of other organs found laterally on the leg) is indeed oriented almost at a right angle to the lines of principal stresses resulting from joint forces generated by muscle activity (Barth and Pickelmann 1975). According to our present experiments, the site of maximum slit compression within a group shifts with load direction even if the slits are arranged in parallel (Fig. 4). This implies that even parallel arrangements could be used to gather directional information from the specific pattern of excitation within the group. There are some slit arrangements in the arachnid exoskeleton, however, which suggest the possibility of load direction analysis on the basis of *diverging* slit axes (Barth and Stagl 1976). Models with three slits, differing in the degree of slit axis divergence, were used to test this effect (Fig. 6).

Deformation. The deformation pattern changes in three main ways with increasing angle β between the slits (Fig. 6). (*i*): The absolute amount of deformation increases with increasing β (as it does with increasing distance between *parallel* slits; Fig. 7). While the compression peaks of slits 1,

[2] The actual range is somewhere between 15°–30° and 150°–165°, respectively. Note limit of resolution due to the stepwise change of the load angle

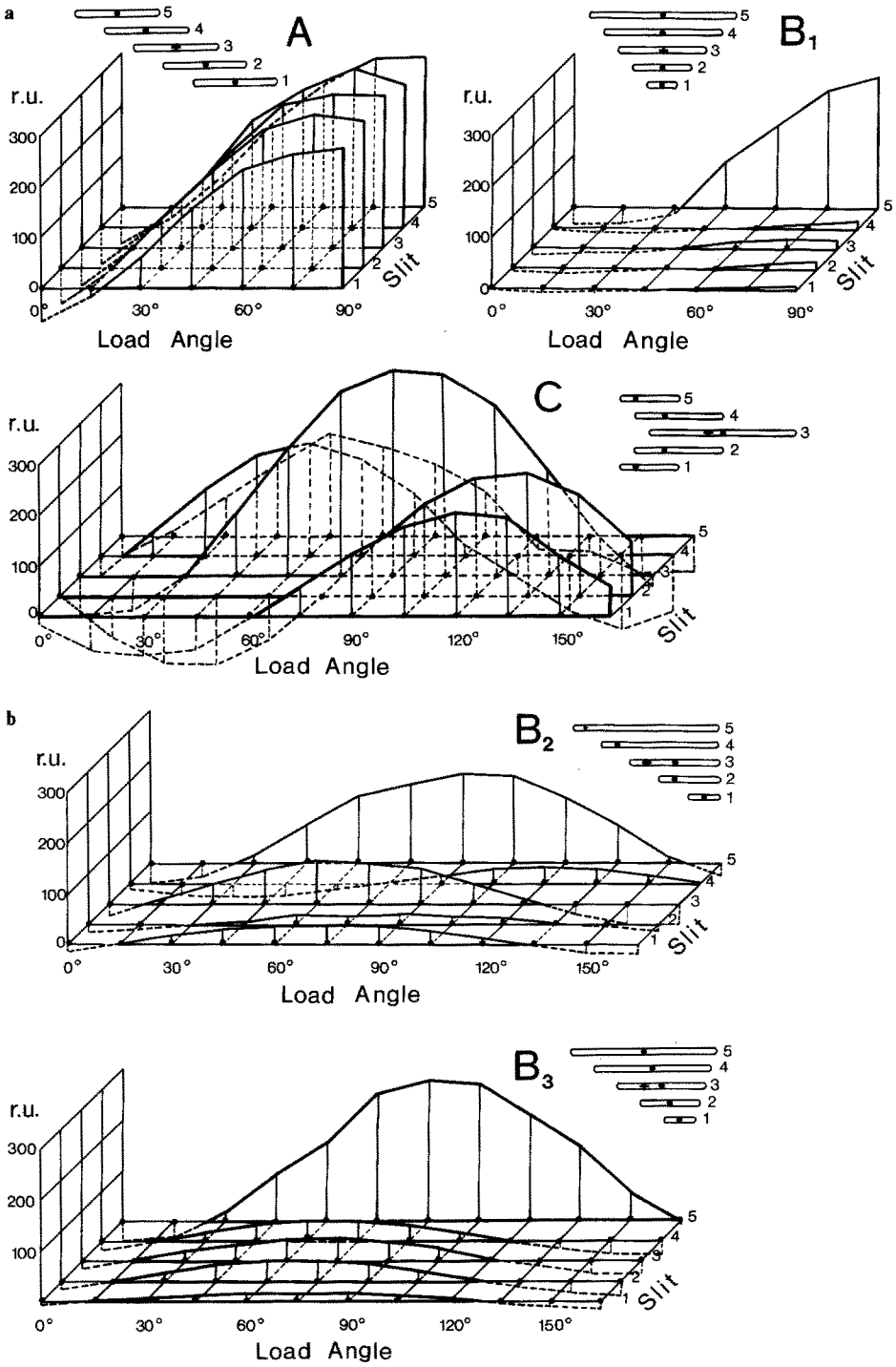

Fig. 5a, b. Deformation of slit regions corresponding to dendrite attachment areas in the originals (here as in other model drawings marked by a filled circle). Load angle α was changed in steps of 15°. Compression values above x-axis, dilatation below it.

2, and 3 measure 8, 1, and 8 (relative units) in the parallel arrangement ($\beta = 0°$), they increase to 14, 5, and 12; 16, 9, and 14; and 20, 16, and 18 at angles β of 15°, 30°, and 45°. (*ii*): It follows from these values that the difference in the degree of maximum deformation between the three slits decreases with increasing angle β. (*iii*): The difference between the load angles resulting in compression peaks in the three slits increases with increasing β. At $\beta = 0°$ all slits are maximally deformed at a load direction of 90°. At $\beta = 15°$, 30°, and 45° the peak deformation of the three slits occurs at different load angles covering a total *range* of 83°, 93°, and 112°, respectively. Corresponding values for the lyriform model organs (Fig. 5a) are all considerably smaller (maximum range 75° in configuration *C*).

2. Distance

In previous studies (Barth and Stagl 1976) a distinction was made between "lyriform or compound slit sense organs", more loosely arranged "groups of single slits", and "isolated slit sensilla". This classification was based on purely morphological grounds using the distance d between neighbouring slits as the main parameter.

From a physiological point of view the interesting ques-

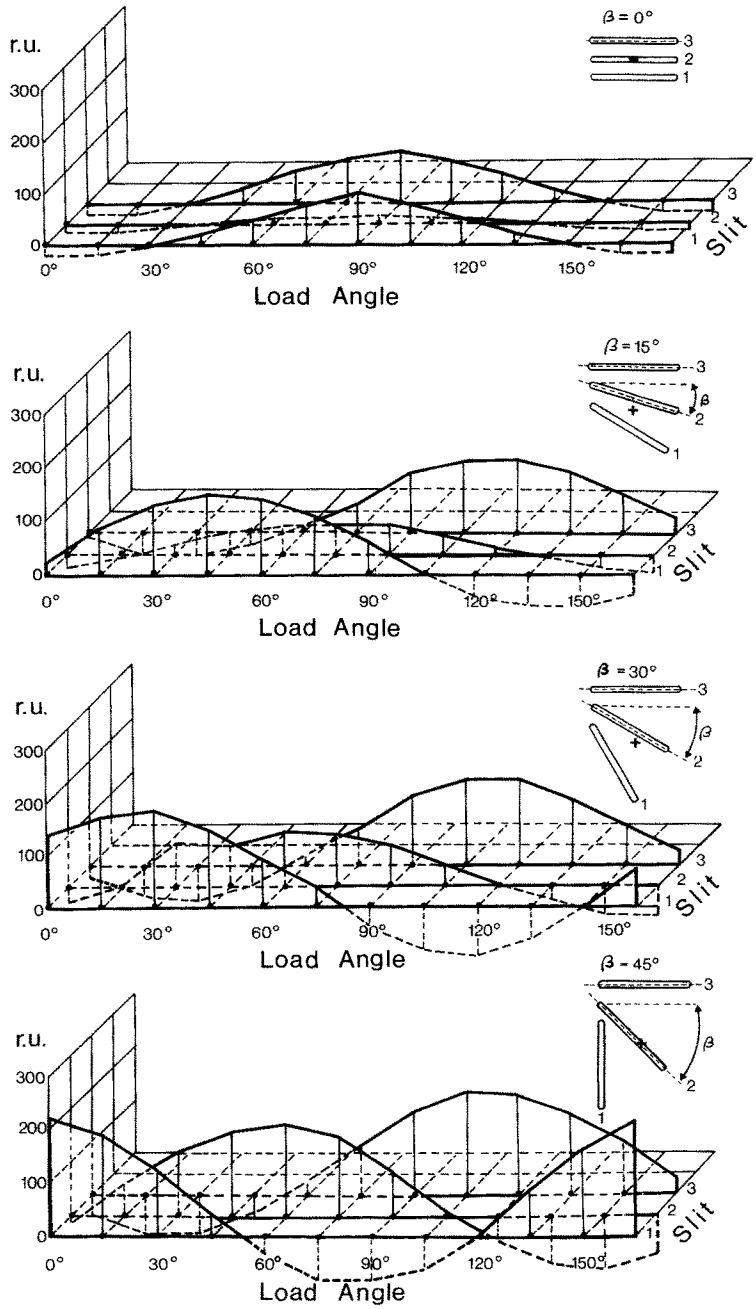

Fig. 6. Slit deformation as a function of both load angle α and the angle β between neighbouring slits in a group of three (1, 2, 3). From above to below β varies between 0° and 45° (see inset on right side). Deformation values refer to center of slit in all cases and are plotted as in Fig. 5.

tion behind this classification is: What is the minimal distance at which neighbouring slits no longer influence each other mechanically? Models with three parallel slits of equal length but varying distance were examined and compared with a model with only one slit.

The deformation of a slit is greatly reduced by the presence of neighbouring slits (Barth and Pickelmann 1975) as long as the distance d between them is equal to or smaller than slit length l (Fig. 7). The effect disappears at $d \sim 1.5 \times l$.

III. Mechanics to explain deformation of compound slit arrangements

The structure of a compound slit organ can be looked at as a hole (corresponding in outline to that of a lyriform organ) traversed by beams (corresponding to the cuticular material separating the slits in the original organ). Deformation of the slits under load results from the deformation of these beams. This in turn is induced by the forces transmitted from the border of the hole to the beam attachments and can be described by either a simple or an S-shaped deflection curve (Fig. 8a, b) (Federle 1980).

There are three component forces acting on the beams: a longitudinal (with respect to beam) force (L), a transverse or shearing force (Q), and a bending moment (Mb) (Fig. 8c). Deformation of the hole periphery shifts the beam attachments either along their long axes due to L, or at right angles due to Q. In addition the attachment may be twisted due to Me ($= Mb$ at attachment site) (Fig. 8d). In beams much longer than high ($l \gg h$) the deflection can be calculated from Mb, provided the deformation is small and the beam remains plane in cross section (e.g. Mönch 1971).

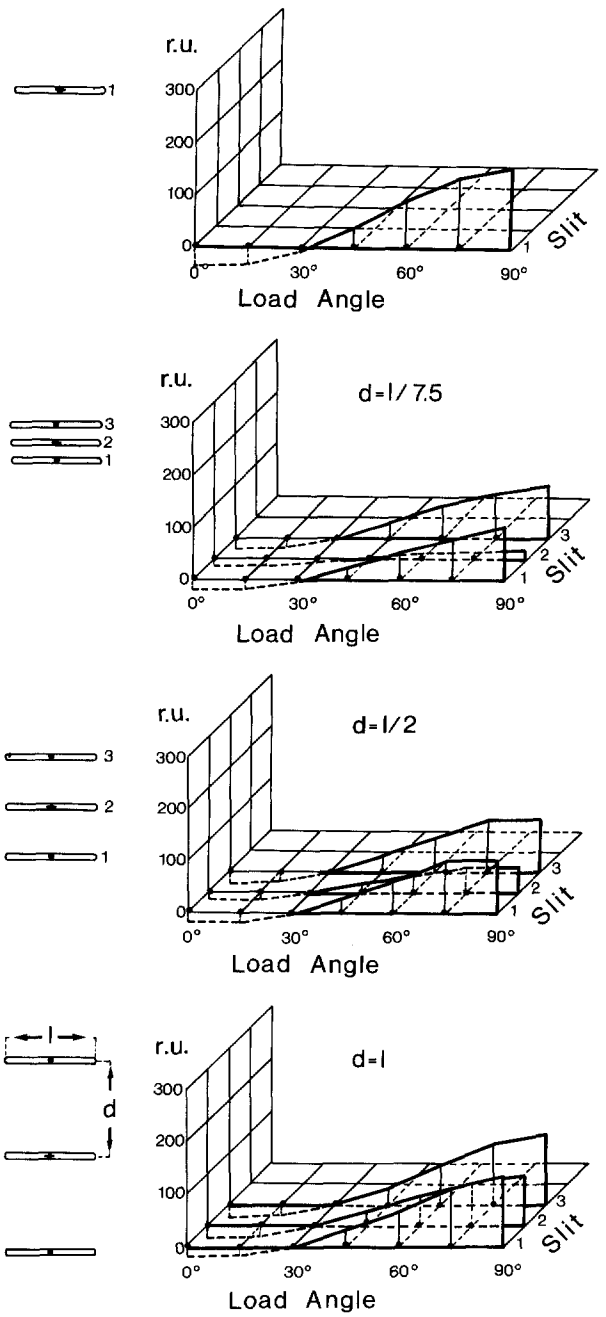

Fig. 7. Slit deformation as a function of both load angle α and distance d between neighbouring slits in a group of three slits (1, 2, 3); l, slit length. For comparison same experiment is shown for a single slit (above). Deformation plotted as in Fig. 5

$$EI\frac{d^2w(x)}{dx^2} = -Mb\,(x) \tag{1}$$

where $Mb\,(x)$ is the bending moment, $w\,(x)$ the deflection at site x, E Young's modulus, and I the geometrical moment of inertia, which in turn is a function of beam thickness d at right angle to plane of load and beam height h (parallel to plane of load) (e.g. Mönch 1971):

$$I=\frac{d\cdot h^3}{12} \tag{2}$$

A photoelastic procedure used to determine statically indeterminate frameworks in engineering, in which the points of zero bending moment are determined (Föppl and Mönch 1972) was applied to see whether the slit deformation, directly measured as described in Sections 1 and 2, can be understood as a consequence of Mb, L, and Q. The procedure is the following: Color slides taken from the isochromatics of the model under load were projected onto a screen and the beams bordering the slits drawn onto tracing paper together with the sites of the points of zero moment and the sites of convergence of the isochromatics of orders 0 to 3 with the beams. First, three steps were taken:

1. The coordinate l_0 of the points of zero moment is calculated from that of the isochromatics of zero order at the upper edge (x_{ou}) and lower edge (x_{ol}) of the beam, respectively:

$$l_0=\frac{x_{ou}+x_{ol}}{2} \tag{3}$$

2. The distance between the convergence of the isochromatics of zero and first order with the beam $(x_1-x_0)=\Delta x$, is used to calculate Q according to

$$Q=\frac{h^2}{6(x_1-x_0)}\cdot f \tag{4}$$

where f is the material fringe value and h the height of the beam. The value for Q derived from this equation is the same as that at the left attachment of the beam (Q_0), except for its opposite sign.

3. Knowing l_0 and Q we can proceed to calculate the *elastic line* of the beam, i.e. its deformation, as a function of Q, of the position of the point of zero bending moment, of the beam dimension, and of the material properties, by double integration of Eq. (1) (Mönch 1971):

$$w=\frac{Q}{6\,EJ}[x^3-3l_0x^2+(3l_0l-l^2)x] \tag{5}$$

Since the cross section of all beams used in the models are identical, the factor $\frac{1}{EJ}$ is constant in the equations for all beams:

$$J=\frac{d\cdot h^3}{12}=\frac{6\cdot 4^3}{12}=32[\mathrm{mm}^4]$$

$$E\approx 3400\ [\mathrm{Nmm}^{-2}]$$

$$\frac{1}{EJ}=9.2\cdot 10^{-6}\ [N^{-1}\mathrm{mm}^{-2}].$$

In fact, the slit deformation measured directly in the models (Δbs) is not exactly the same as that calculated in this way from the deflection curves of the respective beams. The reason for this is a change in the shape of the hole periphery.

Since there is no available theory predicting these changes quantitatively, we introduced a correction factor which minimizes the difference between the calculated and the measured values (Δw–Δbs). A practical case of this procedure using model B_1 as an example is given in the appendix.

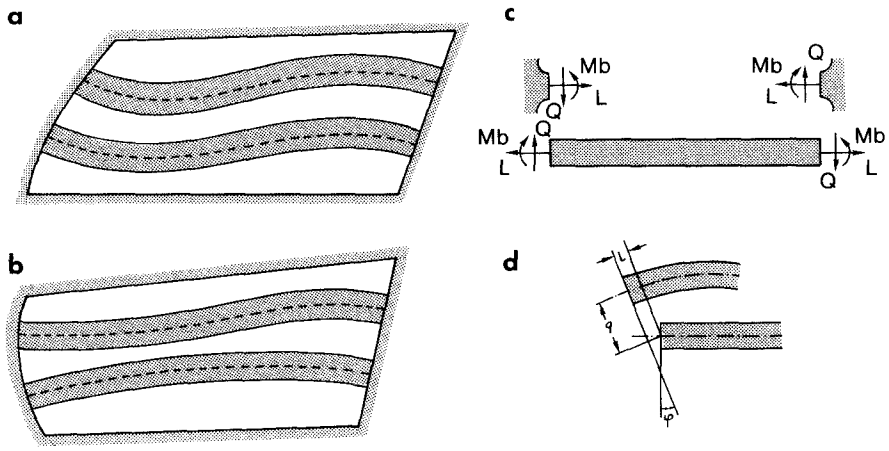

Fig. 8a–d. Deflection of beams traversing a hole by forces introduced by deformation of the hole. **a** S-shaped deflection; **b** simple deflection (lower beam); broken lines give elastic lines of beams. **c** forces acting on a beam in a situation shown by *a* and *b* at their ends: *Q* transverse force, *L* longitudinal force, *Mb* bending moment. **d** displacement of beam by forces shown in *c*: *l*, along long axis of beam due to *L*; *q*, at right angle to long axis of beam due to *Q*; *δ*, angle describing bending of beam at attachment due to *Mb*

D. Discussion

In previous studies on the functional properties of lyriform organs we have concentrated on lyriform organ HS8 in the spider leg tibia as a representative case (Barth and Pickelmann 1975, Barth and Bohnenberger 1978; Bohnenberger 1981, Blickhan et al. 1982; Blickhan 1983, Barth and Blickhan 1984). These studies led to six important conclusions: (*i*) a considerable difference in threshold sensitivity among the slits of the group; (*ii*) an extension of the linear working range (range of high increment sensitivity) by the summation of the linear working ranges of the individual slits composing the group; (*iii*) no obvious frequency tuning of the different slits within the group; (*iv*) coincidence of dendrite attachment site with the area maximally compressed; (*v*) topography of the organ providing high sensitivity due to its orientation roughly at right angles to the stresses occurring at its particular location in the exoskeleton; and (*vi*) a stimulation of this organ only during the stance phase of the stepping cycle during locomotion when strains of up to about $-80\ \mu\epsilon$ occur.

The present experiments on the mechanical implications of different types of slit arrangements point to a number of effects which add important aspects to our knowledge of the functional design of groups of slit sensilla.

For an adequate appreciation of these data both the virtues and limitations of such model studies should be borne in mind. The question of the deformation of slits arranged in groups like lyriform organs is very complex from a technical point of view and no theory is at hand answering it with a set of equations. In addition there are no techniques which would allow measurements in the original organs with the necessary spatial resolution, which is lacking even in such advanced and sensitive procedures as laser-Doppler-vibrometry or the application of Moiré grids. Another obvious difficulty is the loading of the original organs with adequate precision from various directions.

Model studies have previously (Barth 1972a, b; Barth and Pickelmann 1975) turned out to be excellent guides to the main mechanical effects to be expected in the original. They have provided valuable hypotheses otherwise not available. A potential problem with the present models is that they are based on simplified shapes. For obvious reasons not all the details of the originals can be copied. Therefore the data obtained do predict the main mechanical effects of the various types of arrangements; we do not pretend, however, to have an exhaustive picture of all the mechanical implications of all the details found in a particular original organ.

It should be noted that neither effects of the material used in the models nor their size are expected to affect the validity of our data in the above sense (Barth 1972a). There is also no reason to assume qualitatively different results for dynamic load application in the biologically relevant range of frequencies; viscosities may be expected to modify the type of deformation only at frequencies of several kHz (Barth and Pickelmann 1975).

1. Lyriform patterns

The three principal types of slit arrangements chosen for comparison show drastic differences in mechanical behavior, from which we conclude that they are (i) either used for a preferential measurement of different parameters of basically the same stimulus, or (ii) that the stimuli they are exposed to at their respective sites in the exoskeleton vary considerably. In addition, both alternatives may apply.

a) In the *"oblique bar"* model (*A*) deformation of all slits is very similar at all load angles. From a mechanical point of view one would expect neither a big difference in threshold sensitivity among the slits of an original lyriform organ with such an arrangement, nor a working range (load directions resulting in excitation by slit compression) of the entire compound organ much greater than that of its individual, component slits (no range fractionation). In addition, this arrangement does not appear suited to signal load direction: The excitation pattern within the group is more or less the same at all angles; it would be very difficult for the central neurons to distinguish between the effects of stimulus amplitude and direction. What then might be the advantages of this particular configuration? The model studies suggest two possibilities: (i) A particularly *large "field of vision"*, i.e. high sensitivity for strains from a particularly large range of directions. This implies that a large spread of strain directions may be typical of the sites where "oblique bar" arrangements occur (proximal femur of harvestman, distal femur of scorpion, patella of the spider leg; Barth and Stagl 1976). (ii) Based on the similarity of the deformation of the slits, a convergence in the central nervous system of the corresponding sensory inputs from the different channels might be used for an enhancement of absolute sensitivity by a reduction of the *signal-to-noise ratio*.

b) The *triangular configurations* (*B*) impress one with the great difference between the large deformation (high sensitivity) of the longest slit in the periphery and much smaller deformation of the other slits. Here then, a stimulus *amplitude range fractionation* is one important effect. In lyriform organ HS8 the longest slit is outstanding not only with respect to its high sensitivity but also its purely phasic response characteristic, not found in other slits of this organ. Even the relatively small variations among the three triangular models used in the present study lead to considerable changes in the compression ranges and absolute amount of deformation of the four remaining slits. Previous electrophysiological experiments in lyriform organ HS8 have clearly shown that differences in deformation among the slits are reflected by physiological differences in sensitivity. In this organ, threshold sensitivity of only three of the slits (excluding the longest in the group) varied by about 40 dB (Barth and Bohnenberger 1978; Bohnenberger 1981). A correspondingly large variation of strain amplitude is predicted for this and other sites of triangular slit configurations (e.g. trochanter of harvestman, patella and trochanter of spider).

c) Peculiar to the *"heart" configuration* (*C*) is the large spread of the load angles at which the compression of the five slits is highest. This high deformability of all slits, and a correspondingly large change in the deformation pattern within the group with changing load direction, recommend the "heart" configuration as a pattern useful for the analysis of *strain direction,* although at first glance the parallelity of its slits may not seem to be in favour of this conjecture. A corresponding range of strain directions is predicted for those sites in the exoskeleton where this configuration occurs (e.g. laterally on the spider trochanter).

2. Variation of angle between slits

The directionality of a slit sensillum due to its elongated shape suggests still another way of analyzing strain direction. Apart from complex *parallel* arrangements of slits as in the "heart" configuration, the orientation of the slits in different directions can theoretically – and indeed more obviously – be used for that purpose. Although not many cases are known such a spread of slit directions does occur: Within a lyriform organ on the trochanter of the whip spider leg the slit axes diverge by almost 90°; other similar examples are found on the metatarsus of the whip scorpion and on the coxa of the harvestman (Barth and Stagl 1976). On the spider chelicerae two closely neighbouring lyriform organs are oriented at right angles to each other (Barth and Libera 1970). The mechanical effect of such arrangements is clearly demonstrated by our model studies. If they have indeed evolved to measure spatial or temporal variation in strain directions in one particular area of the skeleton the possible advantage over a direction-sensitive parallel arrangement is not obvious. It may be, however, that a larger angular range is covered by a combination of high sensitivity and a smaller number of slits with a lesser degree of overlap of their individual angular working ranges (compare configuration *C* in Fig. 5a with Fig. 6, bottom). It is tempting to compare Fig. 6. ($\beta = 45°$) with the spectral sensitivity curves of the three photoreceptor cell types dividing up the spectrum of visible light into three components in arthorpod and vertebrate color vision. A similar mechanism may be involved in multi-channel analysis of *strain direction,* but has not yet been proved to exist in the original strain detector system. The comparison, however, points to the possible refinement of this unusual mechanosensory system. Recent advances in the biomechanical analysis of the spider exoskeleton, and the development of miniaturized techniques to measure strains in the freely walking animal (Blickhan, Barth and Ficker 1982; Blickhan 1983; Barth and Blickhan 1984), will hopefully enable us to carry the present study one important step further by analyzing directions, amplitudes, and time courses of the strains which occur at the sites in the original skeleton where the slit sense organs represented by the models are found.

E. Appendix

Representative Example for Application of Procedure Outlined in III.

Model B_1, loaded at an angle of $\alpha = 45°$, is taken as a representative case to illustrate our results. Here the hole has the shape of an isosceles triangle. An array of four beams of decreasing lengths results in the formation of five slits. Deformation was measured at four points A to D along their length, dividing them up into five equal sections (Fig. 9). In slit 5 and at measuring points A and D in slit 4 the elastic line cannot be calculated since the condition of $l \gg h$ does not hold here.

From the photoelastic fringe pattern (Fig. 10) the values for l_0 and Q can be determined (Table 1) and used for the calculation of the elastic lines. Beam 1 and beam 2, which determine the deformation of slit 2, are presented as examples together with the excursions found at the measuring points (Table 2).

When calculating slit deformation, the difference of the coordinates of corresponding measuring points in the "upper" and "lower" beam bordering the slit (note differences in beam length) has to be considered (Fig. 9b). Thus deformation of slit 2 at mea-

Table 1.

Beam	x_{00}[mm]	x_{0u}[mm]	l_0[mm]	Δx [mm]	Q_0 [N]	l [mm]
1	8.42	33.38	20.90	14.82	−1.87	38
2	5.46	24.02	14.74	11.70	−2.37	28

For explanation see text

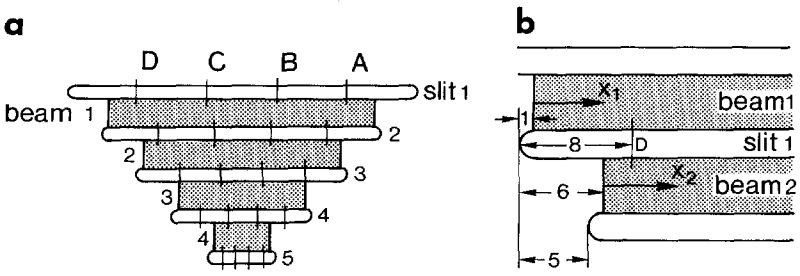

Fig. 9. a Model B1 (see Fig. 4) showing the four beams separating the slits from each other; A, B, C, and D are the sites where slit deformation was measured. **b** determination of the coordinates of measuring sites exemplified by site D of slit 2; while beam 1 at D has the coordinate $x_1 = 7$, the coordinate is $x_2 = 2$ for beam 2

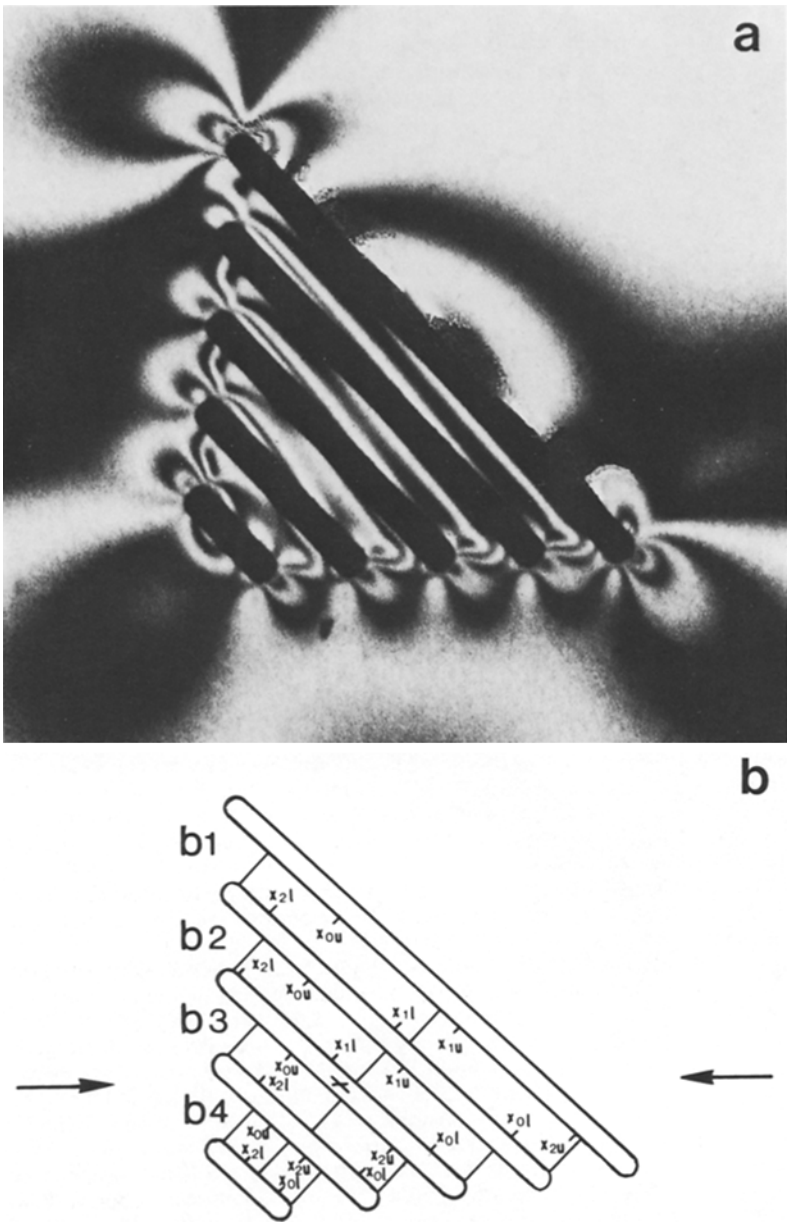

Fig. 10. **a** Isochromatics seen in model B1 if loaded at an angle α of 45°. **b** Schematic representation of **a**, showing the orders of the isochromatics as seen along the beams (b1–b4). For example: x_{2l}, site of isochromatic of second order (2) on lower (l) surface of beam, or x_{1u}, site of isochromatic of first order (1) on upper (u) surface of beam. Lines at a right angle to long axes of beams and roughly in the middle of the beams indicate the site of the point of zero bending moment

Table 2. From equation (5) and the values of table 1
Beam 1

Point	–	–	D	C	B	A	–	–	–	–
x [mm]	9.78	32.05	7	15	23	31	4	14	24	34
w_1 [μm]	12.06	– 4.02	11.25	9.83	1.78	– 3.92	8.24	10.62	0.76	– 3.62

Beam 2

Point	–	–	D	C	B	A	–	–	–	–
x [mm]	6.62	22.85	2	10	18	26	5	11	17	23
w_2 [μm]	5.03	– 2.89	2.74	4.14	– 1.19	– 1.88	4.77	3.61	– 0.54	– 2.89

For explanation see text

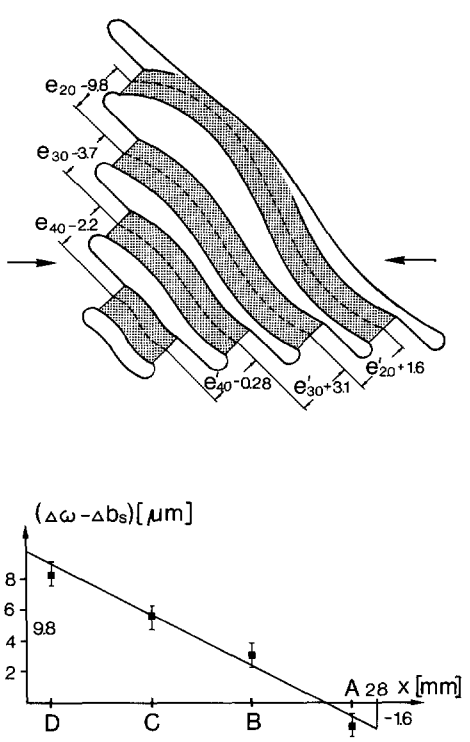

Fig. 11. **a** Deformation of model B1 in experiment shown in Fig. 10a, enlarged by a factor of 1000. *e* and *e'* give displacement of beam attachment sites (lower beam with respect to upper beam). Arrows indicate load direction. **b** Correction introduced to take account of the deformation of the hole periphery under load. If the left attachment site of beam 2 is moved upward by 9.8 μm (Δw–Δbs) and its right one downward by 1.6 μm, the width of the slit 2 as measured directly in the experiment (■) differs from that calculated according to the procedure described in the text (continuous line) by less than 0.8 μm

suring point D is given by the difference between the excursion of beam 2 at site $x_2 = 2$ and that of beam 1 at $x_1 = 7$:

$$\Delta w_D = w_1(7) - w_2(2).$$

The corresponding equations for the other measuring points of slit 2 are

$$\Delta w_C = w_1(15) - w_2(10)$$

$$\Delta w_B = w_1(23) - w_2(18)$$

$$\Delta w_A = w_1(31) - w_2(26).$$

From the two elastic lines the following coordinate differences Δw are calculated for measuring points A to D for slit 2: −2.04, 2.97, 5.69 and 8.51.

The differences between Δw and the change in slit width directly measured in slit 2 (Δbs) with the transducer (Fig. 4) are −1.53, 2.97, 5.59, and 8.34 μm for points A, B, C, and D, respectively (negative values imply slit compression, positive ones slit dilatation). Taking the deformation of the hole periphery into account, however, $\Delta w - \Delta bs$ becomes very small with less than 0.8 μm by shifting the left end of beam 2 upwards by 9.8 μm and its right end downward by 1.6 μm (Fig. 11).

Acknowledgements. This study was supported by grants of the Deutsche Forschungsgemeinschaft to F.G.B. (SFB 45/A2). We are grateful to Miss A. Pohl for excellent technical assistance, to Mrs. H. Hahn for carrying out the drawings, to Dr. E.-A. Seyfarth for valuable comments on the manuscript, and to Mrs. U. Ginsberg for typing it.

References

Barth FG (1972a) Die Physiologie der Spaltsinnesorgane. I. Modellversuche zur Rolle des cuticularen Spaltes beim Reiztransport. J Comp Physiol 78:315–336

Barth FG (1972b) Die Physiologie der Spaltsinnesorgane. II. Funktionelle Morphologie eines Mechanorezeptors. J Comp Physiol 81:159–186

Barth FG (1976) Sensory information from strains in the exoskeleton. In: The insect integument, Hepburn HR (ed). Elsevier, Amsterdam, pp 445–473

Barth FG (1981) Strain detection in the arthropod exoskeleton. In: Sense organs, Laverack MS, Cosens D (eds). Blackie, Glasgow pp 112–141

Barth FG, Libera W (1970) Ein Atlas der Spaltsinnesorgane von *Cupiennius salei* Keys. Chelicerata (Araneae). Z Morphol Tiere 68:343–368

Barth FG, Pickelmann P (1975) Lyriform slit sense organs. Modelling an arthropod mechanoreceptor J Comp Physiol 103:39–54

Barth FG, Wadepuhl M (1975) Slit sense organs on the scorpion leg (*Androctonus australis*, L. Buthidae). J Morphol 145:209–227

Barth FG, Stagl J (1976) The slit sense organs of arachnids. A comparative study of their topography on the walking legs. Zoomorphologie 86:1–23

Bearth FG, Bohnenberger J (1978) Lyriform slit sense organ: threshold and stimulus amplitude ranges in a multi-unit mechanoreceptor. J Comp Physiol 125:37–43

Barth FG, Blickhan R (1984) Mechanoreception. In: Biology of the integument, vol 1, Bereiter-Hahn J, Matoltsy AG, Richards KS ed. Springer, Berlin Heidelberg New York pp 554–582

Blickhan R (1983) Dehnungen im Außenskelett von Spinnen. Ph.D. Thesis Universität Frankfurt a.M.

Blickhan R, Barth FG, Ficker E (1982) Biomechanics in a sensory system. Strain detection in the exoskeleton of arthropods. Proc VII Int Conf Exp Stress Anal, Haifa: 223–234

Bohnenberger J (1981) Matched transfer characteristics of single units in a compound slit sense organ. J Comp Physiol 142:391–402

Federle H-U (1980) Spannungsoptik und mechanische Probleme der Sinnesphysiologie. Zulassungsarbeit Technische Universität München

Föppl L, Mönch E (1972) Praktische Spannungsoptik. 3. Aufl. Springer Berlin Heidelberg New York

Mönch E (1971) Technische Mechanik. R Oldenbourg, München-Wien

Received January 20, 1984